JCB Article

Mice lacking desmocollin 1 show epidermal fragility accompanied by barrier defects and abnormal differentiation

Martyn Chidgey,[1,2] Cord Brakebusch,[3] Erika Gustafsson,[3] Alan Cruchley,[4] Chris Hail,[2] Sarah Kirk,[1] Anita Merritt[1], Alison North,[1] Chris Tselepis,[2] Jane Hewitt,[1] Carolyn Byrne,[1] Reinhard Fassler,[5] and David Garrod[1]

[1]School of Biological Sciences, University of Manchester, Manchester M13 9PT, UK
[2]Division of Medical Sciences, University of Birmingham, Birmingham B15 2TH, UK
[3]Department of Experimental Pathology, Lund University, S-221 85 Lund, Sweden
[4]Clinical and Diagnostic Oral Sciences, Barts and The London, Queen Mary's School of Medicine and Dentistry, London E1 2AT, UK
[5]Department of Molecular Medicine, Max Plank Institute for Biochemistry, D-82152 Martinsried, Germany

The desmosomal cadherin desmocollin (Dsc)1 is expressed in upper epidermis where strong adhesion is required. To investigate its role in vivo, we have genetically engineered mice with a targeted disruption in the *Dsc1* gene. Soon after birth, null mice exhibit flaky skin and a striking punctate epidermal barrier defect. The epidermis is fragile, and acantholysis in the granular layer generates localized lesions, compromising skin barrier function. Neutrophils accumulate in the lesions and further degrade the tissue, causing sloughing (flaking) of lesional epidermis, but rapid wound healing prevents the formation of overt lesions. Null epidermis is hyperproliferative and overexpresses keratins 6 and 16, indicating abnormal differentiation. From 6 wk, null mice develop ulcerating lesions resembling chronic dermatitis. We speculate that ulceration occurs after acantholysis in the fragile epidermis because environmental insults are more stringent and wound healing is less rapid than in neonatal mice. This dermatitis is accompanied by localized hair loss associated with formation of utriculi and dermal cysts, denoting hair follicle degeneration. Possible resemblance of the lesions to human blistering diseases is discussed. These results show that Dsc1 is required for strong adhesion and barrier maintenance in epidermis and contributes to epidermal differentiation.

Introduction

The desmosomal cadherins, desmocollin (Dsc)* and desmoglein (Dsg), mediate adhesion in desmosomes, one of the principal types of intercellular junction in epithelia and cardiac muscle (Chitaev and Troyanovsky, 1997; Marcozzi et al., 1998; Tselepis et al., 1998). Each constitutes a cadherin subfamily that comprises three genetic isoforms (Dsc1, 2, and 3 and Dsg1, 2, and 3) (Buxton et al., 1993). Dscs and Dsgs show tissue-specific expression: Dsc2 and Dsg2 are ubiquitous in desmosome-containing tissues, whereas Dscs 1 and 3 and Dsgs 1 and 3 are restricted to stratified epithelia. In stratified epithelia such as epidermis, the desmosomal cadherins also show differential expression with the "1" isoforms expressed in suprabasal differentiated layers and the "2" and "3" isoforms in more basal layers (Garrod et al., 1996). Dsg1 and 3 and Dsc1 and 3 expression in epidermis is graded reciprocally; the "3" isoforms decrease exponentially from the basal layer as the "1" isoforms increase (Shimizu et al., 1995; North et al., 1996). This implies that their expression patterns may be linked, a possibility also

Address correspondence to David R. Garrod, School of Biological Sciences, 3.239 Stopford Bldg., University of Manchester, Oxford Rd., Manchester M13 9PT, UK. Tel.: 44-161-275-5243. Fax: 44-161-275-3915. E-mail: david.garrod@man.ac.uk

J. Hewitt's present address is Queen's Medical Centre, Genetics Division, Nottingham University, Nottingham NG7 2UH, UK.

A. North's present address is The Rockefeller University, 1230 York Ave., New York, NY 10021.

*Abbreviations used in this paper: DP, desmoplakin; Dsc, desmocollin; Dsg, desmoglein; ES, embryonic stem; K, keratin; PF, pemphigus foliaceus; PG, plakoglobin; RT, reverse transcriptase; TEWL, transepidermal water loss.

Key words: desmosome; desmocollin; epidermis; epidermal barrier; null mutation

suggested by the adjacent chromosomal locations of desmosomal cadherin genes (Hunt et al., 1999). Where they occur together, Dsc1 and Dsc3 are mixed in the same desmosomes. Thus, the Dsc1:Dsc3 ratio increases with stratification, indicating turnover during epidermal differentiation and showing that adhesion at different levels in the epidermis involves different combinations of desmosomal cadherins (North et al., 1996).

Desmosomal adhesion plays an important role in the maintenance of tissue architecture as indicated by the study of human disease and null mutations in mice (Hashimoto et al., 1997; Amagai, 1999; Mahoney et al., 1999; Green and Gaudry, 2000). The loss of expression of desmosomal components in some human carcinomas and the ability of desmosomal expression to block cellular invasion suggests that desmosomes may also have a tumor suppressor function (Garrod, 1995; Shinohara et al., 1998; Tselepis et al., 1998).

A pressing question is whether the differential expression of desmosomal cadherins indicates specific functions for the distinct isoforms. Their graded expression in stratified epithelia implies a possible role in epithelial differentiation. Stratification itself is clearly not dependent on the presence of multiple desmosomal cadherin isoforms, since cornea possesses only Dsc2 and Dsg2 (Messent et al., 2000). In other epithelia, Dsc3 and Dsg3 are associated positionally with cell proliferation and the early stages of differentiation, whereas Dsc1 and Dsg1 are associated with terminal differentiation and keratinization. Thus, the "1" isoforms may provide strong adhesion to resist abrasion in keratinized epithelia, and the "3" isoforms may provide weaker adhesion required for cell proliferation and motility (Legan et al., 1994). Desmosomal cadherins also may be involved in differentiative signaling. Desmosomes participate in both inside-out and outside-in signal transduction (Osada et al., 1997; Wallis et al., 2000). Furthermore, the Dsc and Dsg cytoplasmic domains bind the armadillo proteins plakoglobin (PG) and plakophilin, and PG signaling in the epidermis has been demonstrated, since overexpression affects hair growth (Charpentier et al., 2000). The nuclear location of plakophilins suggests a possible gene regulation role (Hatzfeld, 1999). Thus, either a structural/morphogenetic role and/or a direct or indirect differentiative signaling role for desmosomal cadherins may be envisaged. Mice expressing dominant negative Dsg3 exhibit abnormalities of epidermal proliferation and differentiation (Allen et al., 1996), although Dsg3$^{-/-}$ mice show no obvious abnormalities of epidermal differentiation (Koch et al., 1997).

To approach the question of the function of Dsc isoforms, we have performed targeted ablation of the mouse *Dsc1* gene. This results in a complex phenotype, showing epidermal fragility together with defects of epidermal barrier and differentiation. The epidermis of neonatal mice shows lesions, which resemble those found in IgA pemphigus, and older mice develop chronic dermatitis. These results demonstrate that Dsc1 contributes substantially to epidermal adhesion and function.

Results

Characterization of the *Dsc1* gene

Two λ clones (λC1 and λC4) and a PAC clone (364c17) containing Dsc1 sequence were obtained from library screens. From these, the mouse *Dsc1* gene was characterized in detail. The gene spans ~32 kb and consists of 17 exons (Fig. 1). Exon 10 is the largest (260 bp) and exon 16, which is alternatively

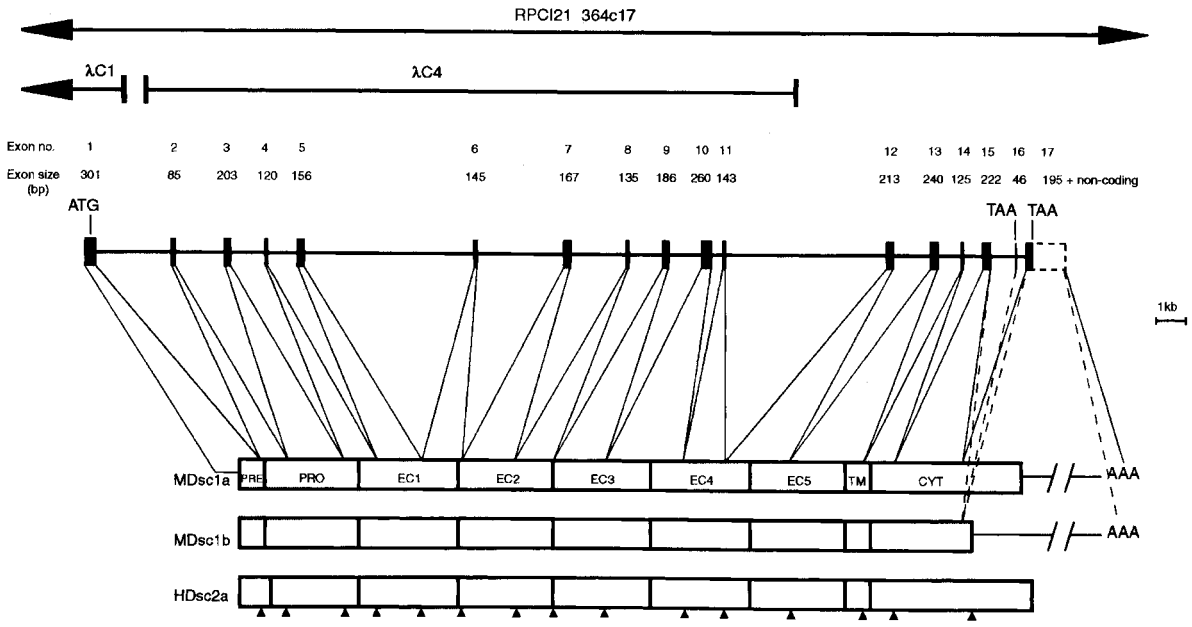

Figure 1. **Exon-intron organization of the murine *Dsc1* gene.** The analysis was conducted using a PAC clone (RPCI21 346c17) and two λ clones (λC1 and λC4). The location of each exon is shown relative to the *Dsc1* gene and a schematic representation of the mouse (M) Dsc1a and Dsc1b proteins. Results from RNase protection assay (unpublished data) suggest that there are no additional 5′ exons. Alternative splicing of RNA can occur; the shorter "b" form of the protein is produced if RNA encoded by exon 16 (which contains an in-frame stop codon) is included in the final message. PRE, signal peptide; PRO, propeptide; EC1-EC5, extracellular homologous repeat domains 1–5; TM, transmembrane domain; CYT, cytoplasmic domain. The locations of introns in human (H) *DSC2* (Greenwood et al., 1997) are shown for comparison and indicated by arrowheads.

Table I. **Exon-intron boundaries of the mouse *Dsc1* gene**

Exon	Exon size	5′ donor	Intron size	3′ acceptor
	bp		*kb*	
1	NC + 63	TTTCTCCTG**gt**gagt	2.6	tttg**ag**GTTCTGGTA
2	85	TAGGCAAAG**gt**gagc	1.7	ctgt**ag**TGAATCTGG
3	203	GAAAAAAAG**gt**aaag	1.1	atat**ag**GTTTTTAGG
4	120	ATTCAGCAG**gt**ctgt	1.1	ttat**ag**ATCCAATCT
5	156	CAATTTTTG**gt**aaga	5.8	ttcc**ag**GTATATGGA
6	145	GCCGATCTG**gt**gagt	3.0	gaac**ag**GAACTTCAG
7	167	GACAGAGAG**gt**aatg	1.9	ttac**ag**AAATGTGAC
8	135	CAAACTTCT**gt**gagt	1.2	cctc**ag**TATACTACA
9	186	AGGCTTAAG**gt**aatg	1.1	aaac**ag**CCACTGAAC
10	260	AGGCTTAAG**gt**aatg	0.4	acct**ag**GTATGAGAT
11	143	CAGATACAG**gt**gagt	5.5	tcct**ag**CTGGCCGAT
12	213	CACAGGATG**gt**aagt	1.3	cttc**ag**GTAAACGTG
13	240	TGCTACTGT**gt**aagt	0.8	ctgt**ag**GCATTTTGT
14	125	GAAGTGACG**gt**aaat	0.7	cttt**ag**GAAGCCAAT
15	222	CTTGGTGAA**gt**aagt	0.9	atac**ag**AAGGTGTAT
16	46	CTTGGTGAA**gt**aagt	0.3	atgt**ag**GAATCCATT
17	195 + NC			

Consensus ag/gt splice sequences are shown in bold. Intron sizes were determined by PCR using primers positioned on flanking exons. NC, noncoding.

spliced to generate the "a" and "b" forms of the protein (Collins et al., 1991), is the smallest (46 bp). Single exons do not correspond to known structural elements such as the extracellular domain internal repeats or the transmembrane or cytoplasmic domains (Fig. 1). All intron-exon borders conform to 5′ and 3′ splice site consensus sequences (Table I). The organization of mouse *Dsc1* shows a striking resemblance to that of other Dsc and classical cadherin genes (Greenwood et al., 1997; Whittock et al., 2000) with exon boundaries highly conserved (Fig. 1).

Generation of *Dsc1*-null mice by homologous recombination

The *Dsc1* gene was disrupted in embryonic stem (ES) cells using the targeting vector shown in Fig. 2 A. On homologous recombination, the vector replaces the translation initiation codon (ATG) and the coding sequence from exon 1 with a neo-cassette. 98 bp at the 3′ end of exon 1 (including 63 bp encoding the start of the Dsc1 signal peptide) and 2.2 kb of intron 1 are replaced by vector DNA.

Four ES cell clones containing a disrupted *Dsc1* allele were identified, and one was used to generate chimeric mice that transmitted the mutated allele to their progeny. Mice heterozygous for the targeted mutation were identified by Southern blotting; wild-type and mutant alleles produced fragments of 20- and 6-kb, respectively (Fig. 2 B). Additional Southern blotting with a probe located 3′ to the homologous sequences in the targeting vector confirmed the presence of the mutated allele in heterozygous mice, and a

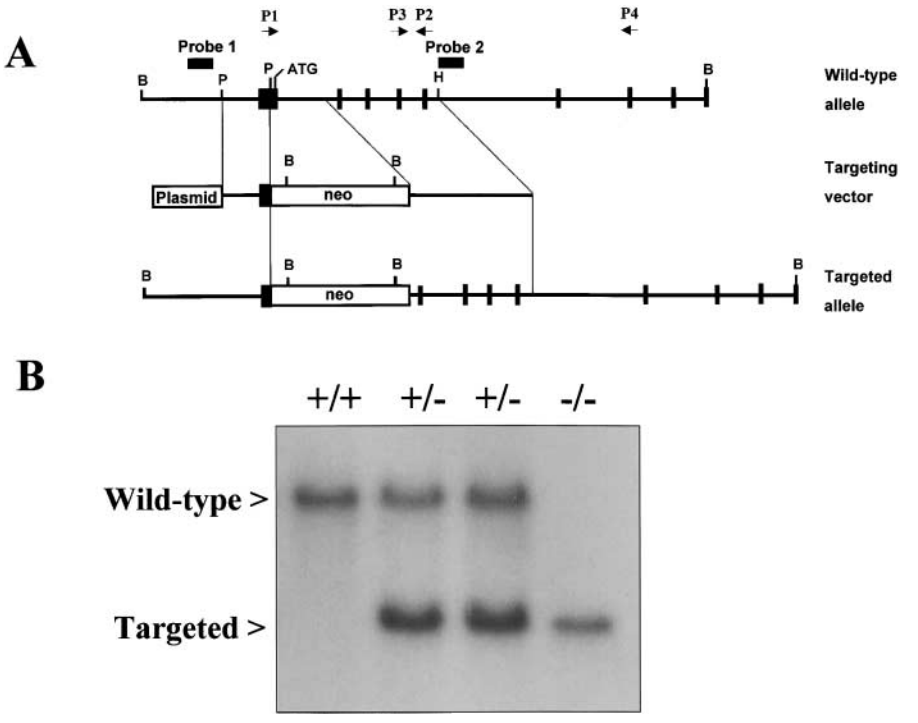

Figure 2. **Targeted disruption of the mouse *Dsc1* gene.** (A) Targeting strategy. The targeting vector consisted of pUC DNA, a neomycin (neo) resistance cassette, and portions of the *Dsc1* gene including 2.1 kb of homology (5′ arm) and 5.2 kb of homology (3′ arm). Filled vertical boxes represent exons. B, BamHI; P, PvuII; H, HindIII. (B) Southern blot analysis of genomic DNA from wild-type (+/+), heterozygous (+/−), and homozygous (−/−) mice. DNA was digested with BamHI, subjected to agarose gel electrophoresis, and transferred to nitocellulose. Wild-type (20 kb) and mutant (6 kb) alleles were detected with probe 1, which hybridized to DNA just outside of the 5′ region of homology. Similarly, probe 2, which hybridized to DNA just outside the 3′ region of homology, detected wild-type (20 kb) and mutant (14 kb) bands (unpublished data).

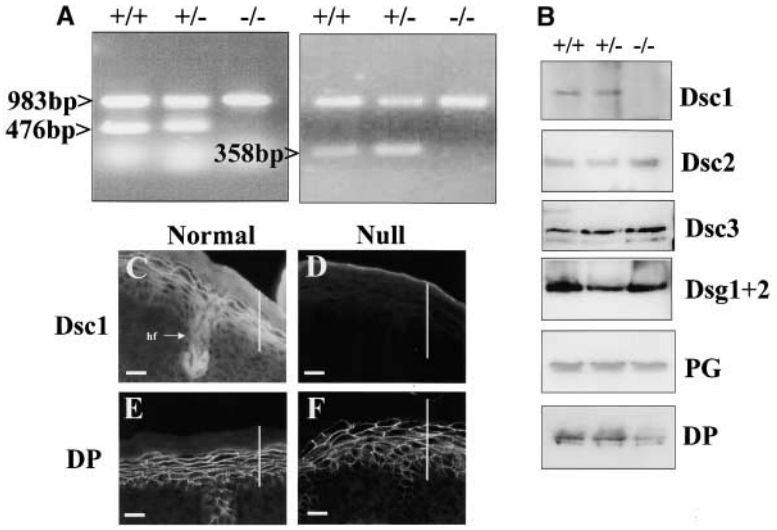

Figure 3. **Expression of desmosomal constituents in Dsc1 mutant mice.** (A) RT-PCR showing absence of Dsc1 message in *Dsc1*$^{-/-}$ mice. Amplification of Dsc1 mRNA was performed using primer pairs P1 and P2 and P3 and P4 (Fig. 2 A) to give 476- and 358-bp products, respectively, in wild-type and heterozygous mice only. Control amplifications using glyceraldehyde-3-phosphate dehydrogenase primers (983-bp product) were performed. (B) Western blot analysis of epidermal extracts using antibodies specific for Dsc1, Dsc2, Dsc3, Dsg1+2, PG, and DP. Equal protein loadings were determined by prior staining with Coomassie brilliant blue. (C–F) Immunofluorescence of epidermis from 2-d-old normal and null mice. Dsc1 is expressed in the epidermis and hair follicles of normal mice (C) but is absent from the skin of null animals (D). DP distribution is unaffected apparently by the absence of Dsc1 and is similar in normal (E) and null mice (F). Vertical bars indicate position of epidermis. Skin samples were taken from the backs of mice. hf, hair follicle. Bars, 25 μm.

neo-derived probe was used to show the presence of only one copy of the neo gene (unpublished data). Heterozygous mice, which could not be distinguished from their wild-type littermates, were crossed and their progeny genotyped. Litter sizes were normal. Of the pups, 26% were wild-type (+/+), 56% were heterozygous (+/−), and 18% were homozygous for the disrupted allele (−/−) ($n = 308$). Thus, the number of homozygous-null offspring was slightly lower than expected. Dsc1 is first expressed at embryonic day (E)13.5 in the outer layers of epidermis (King et al., 1996; Chidgey et al., 1997). To determine whether absence of Dsc1 results in some embryonic mortality, we genotyped E17 embryos from heterozygous crosses. Of these, 28% were wild-type, 43% were heterozygous, and 29% were −/− ($n = 65$). This is a normal Mendelian ratio. These data suggest that some of the *Dsc1*$^{-/-}$ neonates are eaten by the mothers at birth, although no direct evidence for this was found. *Dsc1*$^{-/-}$ mice were fertile: pups from *Dsc1*$^{-/-}$ × *Dsc1*$^{-/-}$ crosses were reared and weaned successfully.

Mice lacking Dsc1 show a neonatal phenotype involving skin, hair, eyes, and growth

Using primers P1 and P2 specific for exons 1 and 5, respectively (Fig. 2 A), full-length Dsc1 mRNA was absent from the epidermis of *Dsc1*$^{-/-}$ mice by reverse transcriptase (RT)-PCR (Fig. 3 A). To confirm the absence of a 5′-truncated message, RT-PCR was performed using primers P3 and P4 specific for exons 4 and 7, respectively (Fig. 2 A). No evidence for a truncated message was found (Fig. 3 A). Primer P3 hybridizes to DNA downstream of that encoding the beginning of the mature protein. Hence, it is extremely unlikely that a truncated message smaller than that which would be detected by primer pair P3-P4 would produce a functional protein. Western blotting with a polyclonal antibody raised against a substantial portion of the extracellular domain of Dsc1 (North et al., 1996) showed absence of the protein from *Dsc1*$^{-/-}$ epidermis (Fig. 3 B). No evidence for the production of a truncated protein was found. Western blotting also showed no clear differences in expression of other desmosomal components (Dsc2, Dsc3, Dsg1+2, PG, desmoplakin [DP]) (Fig. 3 B). Immunofluorescence demonstrated absence of Dsc1 from *Dsc1*$^{-/-}$

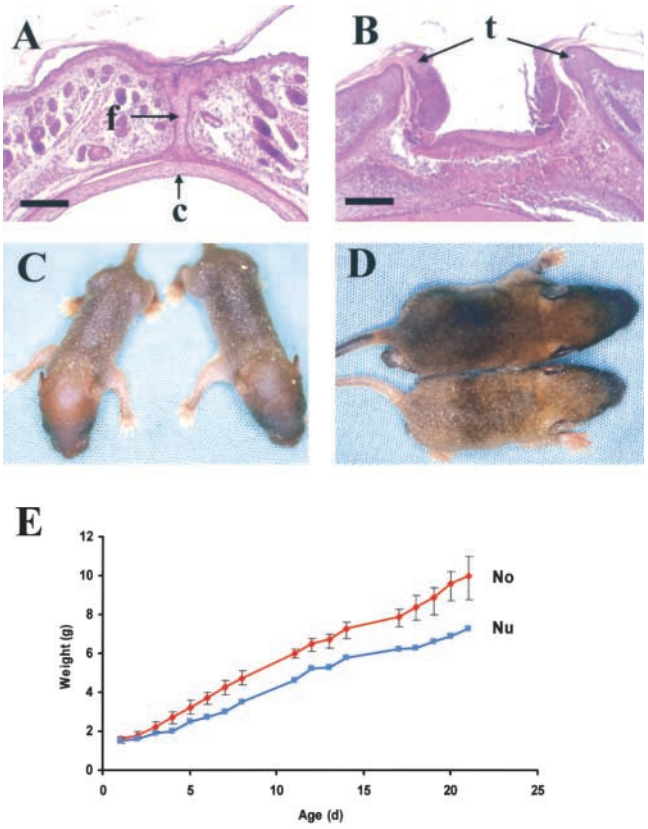

Figure 4. **Eye, skin, and growth abnormalities in Dsc1-null mice.** (A) Eyelids from a 2-d-old normal mouse. f, fused eyelid epidermis; c, cornea. (B) Eyelids from a *Dsc1*$^{-/-}$ littermate showing a failure of eyelid fusion, inflammation, and corneal damage. t, eyelid tips which have failed to fuse. (C) Flaky skin in two null mice at 2-d-old. At this age, null mice were indistinguishable in size from their normal littermates. (D) Flaky skin and characteristic runted appearance in an 8-d-old null mouse (bottom animal) when compared with a normal littermate (top animal). (E) Delayed weight gain in Dsc1-null mice. Results from a typical litter consisting of nine pups in which a null (Nu) mouse and its normal (No) littermates were born with equal weights, but at weaning (21 d) the null mouse weighed 30% less than the average of the others. Bars represent range of weights of normal littermates. 10 litters were examined with similar results. Bars, 150 μm.

epidermis and the inner root sheaths of hair follicles (Fig. 3, C and D). Other desmosomal components were unchanged (DP shown) (Fig. 3, E and F).

At birth, homozygous mice were generally indistinguishable from their littermates, but 10% were born with one or both eyes open (Fig. 4, A and B). Failure of eyelid fusion led to corneal damage and inflammation and corneal opacity or micropthalmia later in life. From day 2, null mice could be distinguished from their normal (i.e., $Dsc1^{+/+}$ and $Dsc1^{+/-}$) littermates because null skin was covered in white flakes or scales (Fig. 4, C and D).

Although born at the same size, null mice usually grew less rapidly (Fig. 4 D), and by weaning (21 d) they were ~30% smaller than littermates (Fig. 4 E; see Fig. 9 A). Slower growth was not due to an obvious feeding defect. The guts of null mice had milk in their stomachs and a normal appearance throughout their length, indicating that the food was processed normally. Dsc1 is expressed in mouse tongue, hard palate, esophagus, and forestomach (King et al., 1996, 1997), but histological examination of these tissues from null mice revealed no abnormalities of the epithelia. Inspection of the oral cavities of null pups revealed no blistering of epithelia. Thus, $Dsc1^{-/-}$ mice did not show the type of oral blistering defects responsible for feeding defects and small size in $Dsg3^{-/-}$ mice (Koch et al., 1997). Of null animals, 10% remained runted, but others caught up after weaning so that by 3 mo there was no significant difference in weight between them and normal mice. Thus, although growth was slower adult size was not generally affected.

Dsc1 is expressed in the Hassal bodies of human thymus (Nuber et al., 1996). To test for an effect on thymus, we examined it histologically and counted numbers of peripheral blood T cells labeled with antibodies to CD4 and CD8 by flow cytometry. No differences were found.

Mice lacking Dsc1 show abnormal epidermal proliferation and differentiation

Histology showed that the epidermis of $Dsc1^{-/-}$ mice was considerably thicker than that of littermates. Normal epidermis consisted of two to three cell layers below the cornified layer, but that of null mice had one, two, or three additional layers, and thickening was found at all body sites. At 2 d, thickening was principally in the spinous layer (Fig. 3, E and F, and Fig. 5, A and B), although localized hyperkeratosis and parakeratosis were also seen (Fig. 5 C). The epidermal cells often but not always appeared larger in the thickened null epidermis (Fig. 5, A and B, compared with Fig. 3, E and F). To determine whether epidermal thickening was due to increased cell proliferation, we examined the skin from null and normal mice using an antibody against Ki67. Proliferating cells were infrequent (3% of all epidermal nuclei) in normal mouse skin and found exclusively in the basal cell layer (Fig. 5 D). By contrast, in null mouse epidermis keratinocytes with nuclear Ki67 were extremely abundant (33% of all epidermal nuclei) and observed frequently in suprabasal layers (Fig. 5 E).

To investigate the effects of the null mutation on epidermal differentiation, we examined the expression of differentiation markers by immunofluorescence. No differences between normal and null epidermis from 2-d-old animals were observed in the distributions of the basal markers P-cadherin (Fig. 6, A and B), β_4-integrin (Fig. 6, D and E), and keratin 5 (unpublished data). Early markers of terminal differentiation (keratin [K]1, involucrin) and a marker for late epidermal differentiation (filaggrin) were normal in 2-d-old null mice (unpublished data). However, a striking difference in the hyperproliferation markers keratins 6 and 16 was found. In normal 2-d epidermis, expression of K6 was restricted mostly to hair follicles (Fig. 6 G), although localized interfollicular epidermal staining was found occasionally. In null epidermis, K6 was present in both hair follicles and interfollicular epidermis (Fig. 6 H). Such K6 expression was observed at all body sites but was patchy locally: in some places expression was present throughout interfollicular epidermis but was absent from others. In normal epidermis, K16 was expressed in hair follicles, and superficial staining was present in suprabasal interfollicular epidermis (Fig. 6 J). In null animals, expression of the protein was upregulated and detected in all cell layers of interfollicular epidermis (Fig. 6 K).

In later life, null mice were susceptible to skin ulceration (see below). In lesioned epidermis from adult null mice,

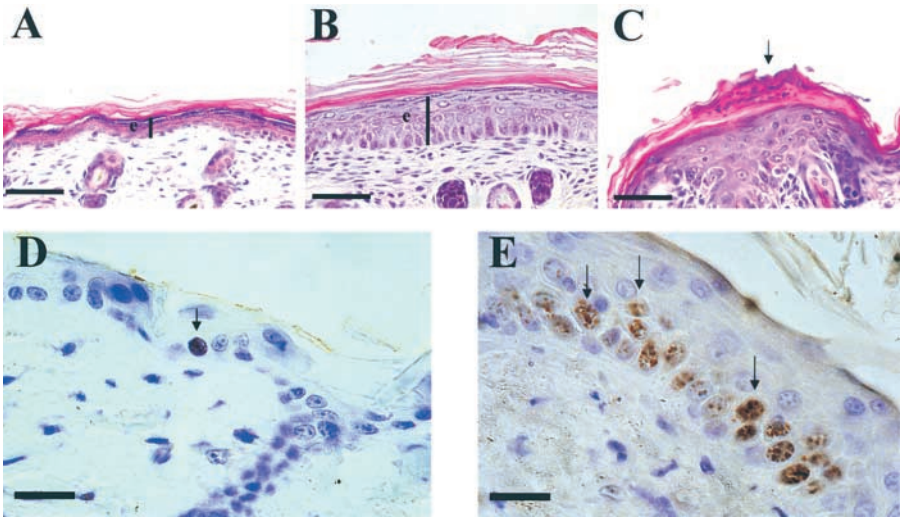

Figure 5. **Hyperplasia and increased cell proliferation in Dsc1-deficient epidermis.** (A) Epidermis from a 2-d-old normal mouse. (B) Epidermis from a $Dsc1^{-/-}$ littermate showing hyperplasia. Bars (e) indicate thickness of living layers of epidermis. (C) Epidermis from a Dsc1-null mouse showing localized hyperkeratosis and parakeratosis (retention of nuclei in the cornified layer) (arrow). (D) Expression of Ki67 in the epidermis in a normal mouse. (E) Ki67 staining in the epidermis of a $Dsc1^{-/-}$ mouse. Only one proliferating cell located in the basal layer is present in D (arrow), whereas in E almost all of the cells in the basal layer and numerous suprabasal cells (arrows) are undergoing cell division. A–C show head skin; D and E show back skin. Bars: (A–C) 100 μm; (D and E) 50 μm.

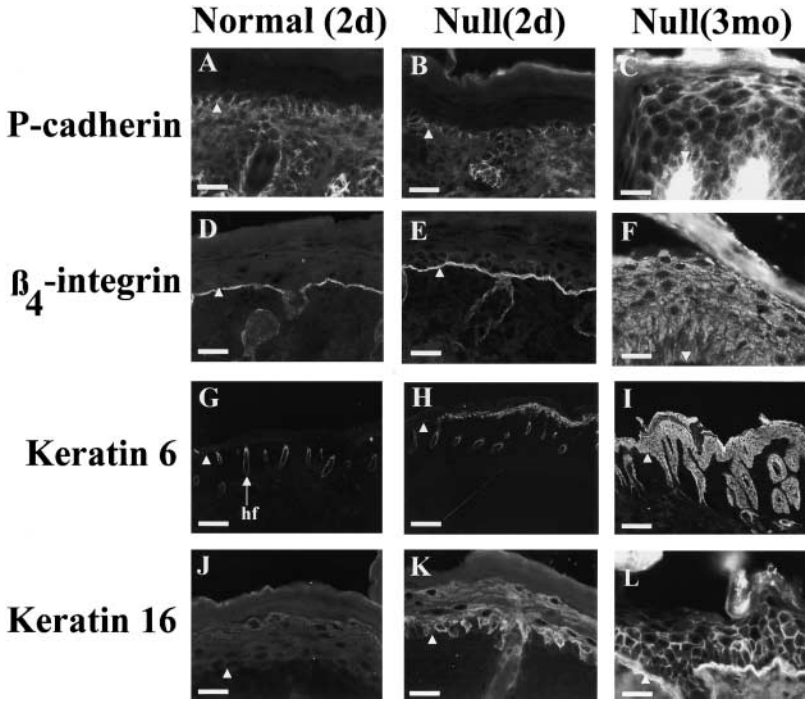

Figure 6. **Immunofluorescence of differentiation markers in Dsc1-null mice.** Distribution of P-cadherin in normal (A) and null (B) 2-d-old animals. In both cases, expression is confined to the basal cell layer and hair follicles. However, dramatic upregulation of P-cadherin is found in lesioned epidermis from adult (~3-mo-old) null animals (C). Similarly, distribution of β_4-integrin expression is similar in normal (D) and null (E) 2-d epidermis but is increased dramatically in all cell layers of lesioned epidermis from older null mice (F). Keratin 6 is expressed in hair follicles of normal mice (G), whereas in unlesioned epidermis from 2-d-old null animals it is found both in hair follicles and interfollicular epidermis (H). Dramatic upregulation of keratin 6 is found in lesioned epidermis from adult null animals (I). In normal animals, superficial keratin 16 staining is detected in suprabasal layers (J), whereas in null mice it is expressed strongly throughout the epidermis including the basal cell layer in both nonlesioned (K) and lesioned epidermis (L). Arrowheads indicate the basement membrane. All micrographs show back skin. Bars: (A–F and J–L) 25 μm; (G–I) 150 μm.

basal layer markers were expressed in all cell layers (Fig. 6, C and F). There were no differences in the distributions of K1 and filaggrin. Both K6 (Fig. 6 I) and K16 (Fig. 6 L) were found throughout lesioned epidermis.

Cornified envelope formation is an important aspect of epidermal terminal differentiation. Because a Dsc, Dsc3, has been reported as a component of cornified envelopes (Robinson et al., 1997) and because *Dsc1*$^{-/-}$ mice showed abnormal epidermal differentiation, we compared cornified envelopes from the epidermis of null and wild-type mice. No difference in appearance was detectable.

Dsc1 deficiency produces epidermal fragility with localized loss of barrier activity

Two observations from neonatal mice suggested that the epidermis of *Dsc1*$^{-/-}$ mice is more fragile than that of littermates. First, histology revealed splits in the epidermis. Such acantholysis, which was absent from normal epidermis, occurred within the granular layer between the granular and spinous layers (Fig. 7 A) or between the cornified and granular layers. Second, when we attempted to isolate the epidermis from 2-d-old mice we found that null epidermis could only be removed in small pieces, whereas normal epidermis remained in sheets (Fig. 7, B and C).

We determined the effects of eliminating Dsc1 on desmosome ultrastructure in the epidermis. No abnormalities in the structure or number of desmosomes were found, including those at the level of the upper spinous and granular layers where Dsc1 expression is strongest (Fig. 7, D and E). Similarly no changes in desmosomes in the inner root sheaths of hair follicles were apparent (unpublished data). By EM, epidermal splits showed an absence of cell lysis and desmosomes, indicating that splitting occurred because of weakened adhesion (Fig. 7 F).

We speculated that flaky skin and epidermal fragility could lead to defects in the skin barrier. To examine this, barrier activity was tested by dye penetration assays (Hardman et al., 1998; Marshall et al., 2000). E17 embryos showed no staining so the barrier was complete before birth. Also, 2-d-old normal mice stayed uniformly white, indicating complete barrier formation (unpublished data; Hardman et al., 1998). However, 2-d-old null mice showed numerous dark spots, indicating localized loss of barrier function (Fig. 8 A). These lesions were not left-right symmetric, indicating that environmental factors contributed to their formation.

Histology of stained spots showed that formation and repair of the lesions could be viewed as sequential events. Early lesions appear in the subcorneal region of epidermis as localized accumulations of neutrophils (Fig. 8, B and C). Such lesions bear a striking resemblance to those found in the subcorneal pustular dermatosis form of IgA pemphigus (Fig. 8 B compared with Fig. 1 c in Hashimoto et al., 1997). Next, the epidermis is degraded by inflammatory cells and partially detaches from the underlying matrix (Fig. 8, D and E), allowing penetration of dye (Fig. 8 A). Concurrently, epithelial cell migration into the wound site is initiated (Fig. 8 E). Finally, when wound healing is complete the damaged epidermis detaches from the underlying tissue, leaving behind an intact newly formed barrier (Fig. 8 F).

To quantify loss of barrier function, body skin from 2-d-old animals was used for determination of permeability constants (Kp) to water and mannitol, a marker for paracellular permeability (Fig. 8 G). Values for Kp were significantly higher ($p < 0.05$) for null animals. The null skin Kp for mannitol was twice that for normal skin, and permeability to water was increased 1.6-fold (Fig. 8 G). These results indicate that absence of Dsc1 causes a defect in the skin barrier.

To examine transepidermal water loss (TEWL), measurements were performed on 25 wild-type and 29 null pups. These gave values of 5.2 mg/h and 6.3 mg/h, respectively.

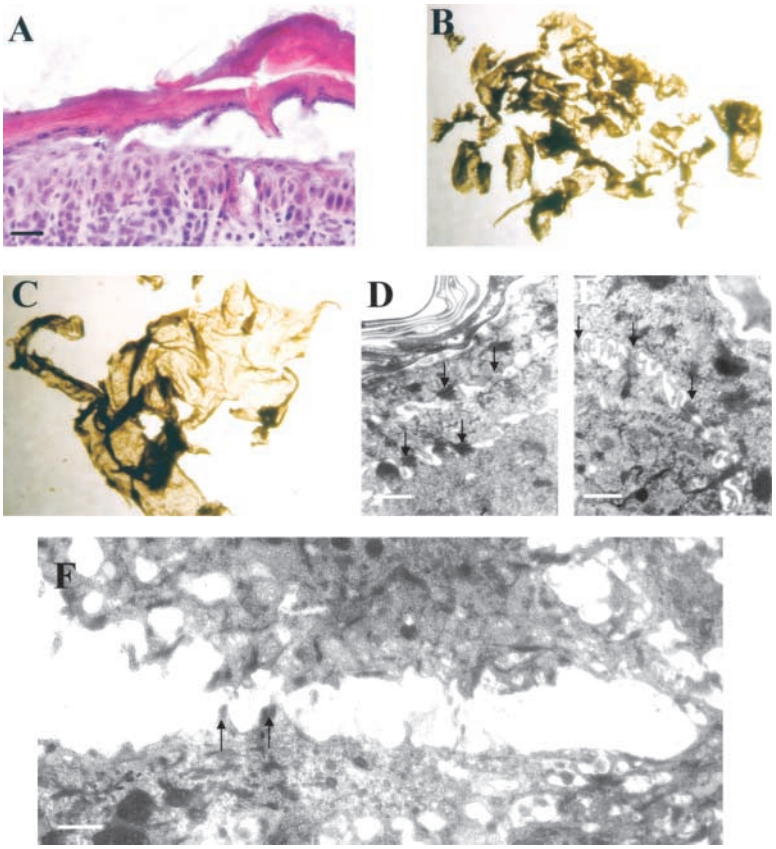

Figure 7. **Absence of Dsc1 weakens adhesion in upper epidermis despite the presence of ultrastructurally normal desmosomes.** (A) Epidermis from a 2-d-old null mouse showing hyperplasia and acantholysis. The granular layer appears to be separating from the upper spinous layer. (B) Epidermis isolated from a 2-d-old *Dsc1*$^{-/-}$-null mouse after treatment with EDTA showing that the tissue fragments allow only small pieces of epidermis to be separated from the dermis. (C) Epidermis isolated using the same technique from a normal littermate. (D) Ultrastructure of outer layers of epidermis from a normal mouse showing desmosomes (arrows). (E) Ultrastructure of outer layers of epidermis from a Dsc1-null mouse with desmosomes (arrows) of a normal appearance. (F) Ultrastructure of lesional epithelium in a Dsc1-null mouse showing splitting between cells and an absence of cell lysis. Arrows indicate possible remains of split desmosomes. All samples were from back skin. Bars: (A) 20 μm; (D and E) 1 μm; (F) 2 μm.

Thus, TEWL for null mice was ~1.2-fold greater than for wild-type controls ($p = 0.02$).

Dsc1-null mice develop alopecia and chronic dermatitis

The coats of adult null mice had a slightly untidy ruffled appearance (Fig. 9 A). Their pelage hairs were indistinguishable from those of normal littermates with similar distributions of awls, auchenes, zig-zags, and guard hairs, and whiskers appeared normal. In later life (usually manifesting at between 1 and 2 mo), >90% of null mice suffered hair loss and skin ulceration (Fig. 9, B and C). Hair loss was most common ventrally (Fig. 9 B), but some individuals had bald patches on the back, and two mice showed more general hair loss. Ulceration was most common around the muzzle (Fig. 9 C) but was also found elsewhere on the head, ventrally, or on the back. Muzzle lesions appeared between 6 wk and 6 mo, and affected mice were killed. Mice that were caged alone developed the same phenotype.

To investigate the mechanism of hair loss, we examined hair follicles at various stages of the hair cycle. No striking abnormalities were found at 5 (first anagen), 18 (catagen), 21 (telogen), and 28 d (second anagen). Tape stripping of the coats detached no more hairs from null than from normal mice, indicating that hairs were firmly anchored in null follicles.

In older animals, severe epidermal and follicular hyperplasia was observed in ulcerated areas of skin (Fig. 9 C) and occasionally in uninvolved skin. In hyperplastic epidermis, substantial thickening of the stratum corneum (hyperkeratosis) was observed (Fig. 9, D and E). Normally differentiated hair follicles were absent and replaced by large comedo-like malformations (utriculi) and cysts (Fig. 9, D and F). Such structures characteristically result from disintegration of hair follicles, suggesting that the observed alopecia is a result of hyperplasia and loss of normal hair follicle morphology. In some ulcerated regions, the epidermis was lost completely (Fig. 9 E). Severe inflammation and tissue necrosis were also observed. The most striking examples of focal overgrowth of keratinocytes were found in both apparently normal and ulcerated whisker pads, which showed a marked papillomatous nature (Fig. 9, G compared with H) with hyperkeratosis and parakeratosis. No evidence of malignant conversion was found. *Dsc1*-null mice were diagnosed as suffering from chronic dermatitis.

Discussion

Deletion of *Dsc1* has two consequences for epidermis. First, weakened adhesion gives rise to epidermal fragility and acantholysis. In early life, this produces a striking localized loss of barrier function and skin flaking. In older mice, substantial ulceration occurs. Second, epidermal differentiation is abnormal, manifested as epidermal hyperproliferation and thickening, an upregulation of keratin 6 and 16 expression, and localized hyperkeratosis and parakeratosis.

Absence of Dsc1 did not result in any alteration in the structure of desmosomes in the upper epidermis, but acantholysis indicates that they are more weakly adhesive than in normal mice, presumably relying on other Dscs for their structure and adhesion. However, there was also no apparent alteration in the expression of other desmosomal components, a result similar to that found in *Dsg3*$^{-/-}$ mice (Koch et al., 1997). Thus, although the expression of the glycopro-

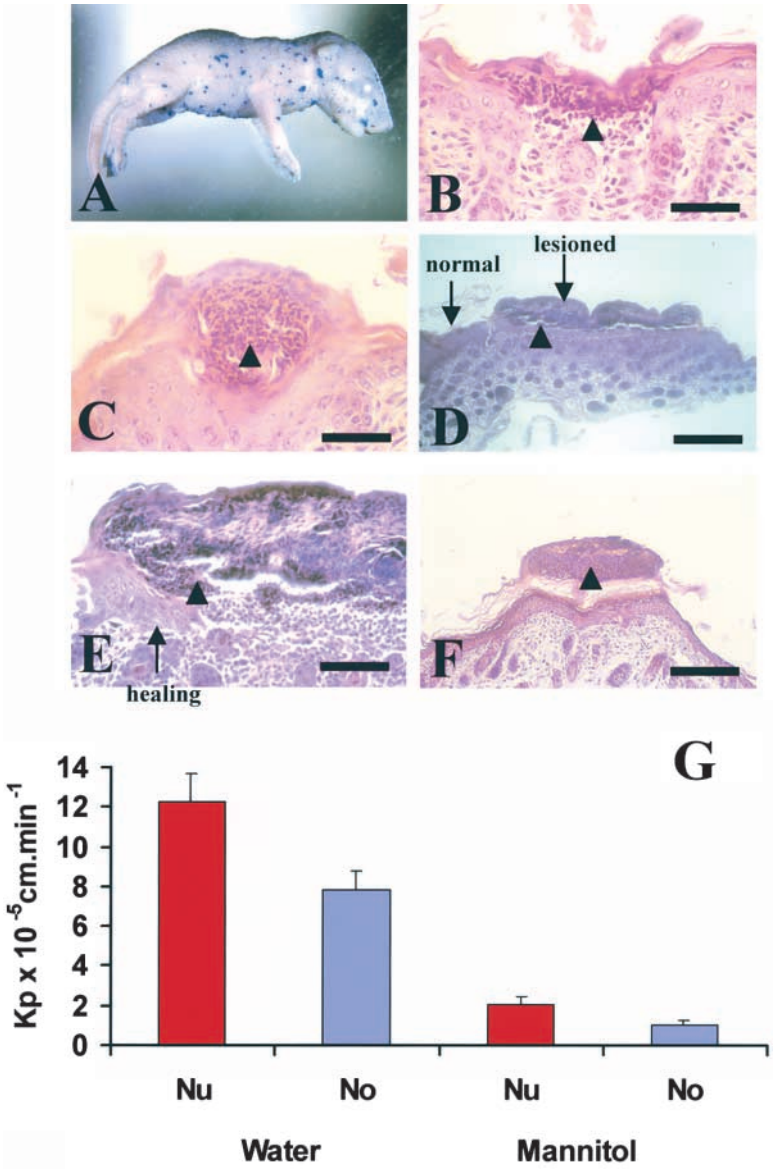

Figure 8. **Dsc1-null mice have skin barrier defects.** (A) Localized breaches in the skin barrier allow penetration of dye into the epidermis of a null mouse but not its normal littermate, which was completely white, that is, unstained (unpublished data). (B and C) Early lesions in the skin of 2-d-old null mice showing infiltration of epidermis with polymorphonuclear cells (neutrophils). (D) More developed lesion in 2-d epidermis showing epidermal degradation and detachment from the underlying dermis. (E) Higher magnification showing epithelial cell migration from intact tissue into wound site. (F) Healed lesion in the epidermis of a 2-d-old null mouse. The damaged epidermis has completely detached from the underlying healed tissue. Arrowheads indicate polymorphonuclear cells. (G) Measurement of permeability coefficients (Kp) for water and mannitol under passive conditions show that skin from 2-d-old null mice is more permeable to both water and solutes ($p < 0.05$ in both cases) than that of a normal littermate. Nu, null; No, normal. Bars: (B, C, and E) 25 μm; (D and F) 100 μm.

tein genes has been postulated to be linked (North et al., 1996; King et al., 1997) two examples of gene deletion have not resulted in compensatory upregulation of other family members.

The acantholysis in the upper epidermis in *Dsc1*$^{-/-}$ resembles that seen in the human autoimmune blistering disease pemphigus foliceus (PF) (Mahoney et al., 1999), reflecting the similar epidermal expression patterns of Dsc1 and the PF antigen Dsg1. In PF, acantholysis results from binding of IgG autoantibody to the extracellular domain of Dsg1. There is no evidence for the involvement of antibodies to Dsc1 in PF. Subsequently, the localized acantholytic lesions in *Dsc1*$^{-/-}$ mice become infiltrated with polymorphonuclear cells (neutrophils). The lesions are reminiscent of those seen in the human subcorneal form of IgA pemphigus in which IgA autoantibodies to Dsc1 bind to the peripheries of epidermal keratinocytes (Hashimoto et al., 1997). No evidence for the pathogenicity of these antibodies has yet emerged. Whether the resemblance between the lesions is coincidental or has significance for the etiology of IgA pemphigus awaits clarification.

Although the acantholytic lesions appear similar, those in young *Dsc1*$^{-/-}$ mice do not progress. In the human diseases, red encrusted lesions are characteristic of PF and red pustular blisters are characteristic of IgA pemphigus, yet the epidermis of the mice remain unblemished apart from the appearance of white flakes. We suggest that skin lesions in young mice are triggered by local acantholysis but do not progress because wound healing is rapid. Reepithelialization of wounds takes ~50% longer in 6–8-wk-old mice than in neonatal mice (Whitby and Ferguson, 1991). This difference in the rate of wound healing can account for the difference in severity between the lesions of neonatal mice and older mice. The environmental insults experienced by older animals are more severe than in young mice during suckling. Repeated insults, especially scratching, give rise to lesions in the epidermis that cannot be healed as rapidly as in neonatal animals. Exacerbation of lesions leads to ulceration and chronic dermatitis, which in this case is a proliferative response of the epidermis to damage. Similar lesions have been found in *Dsg3*$^{-/-}$ mice (Amagai et al., 2000).

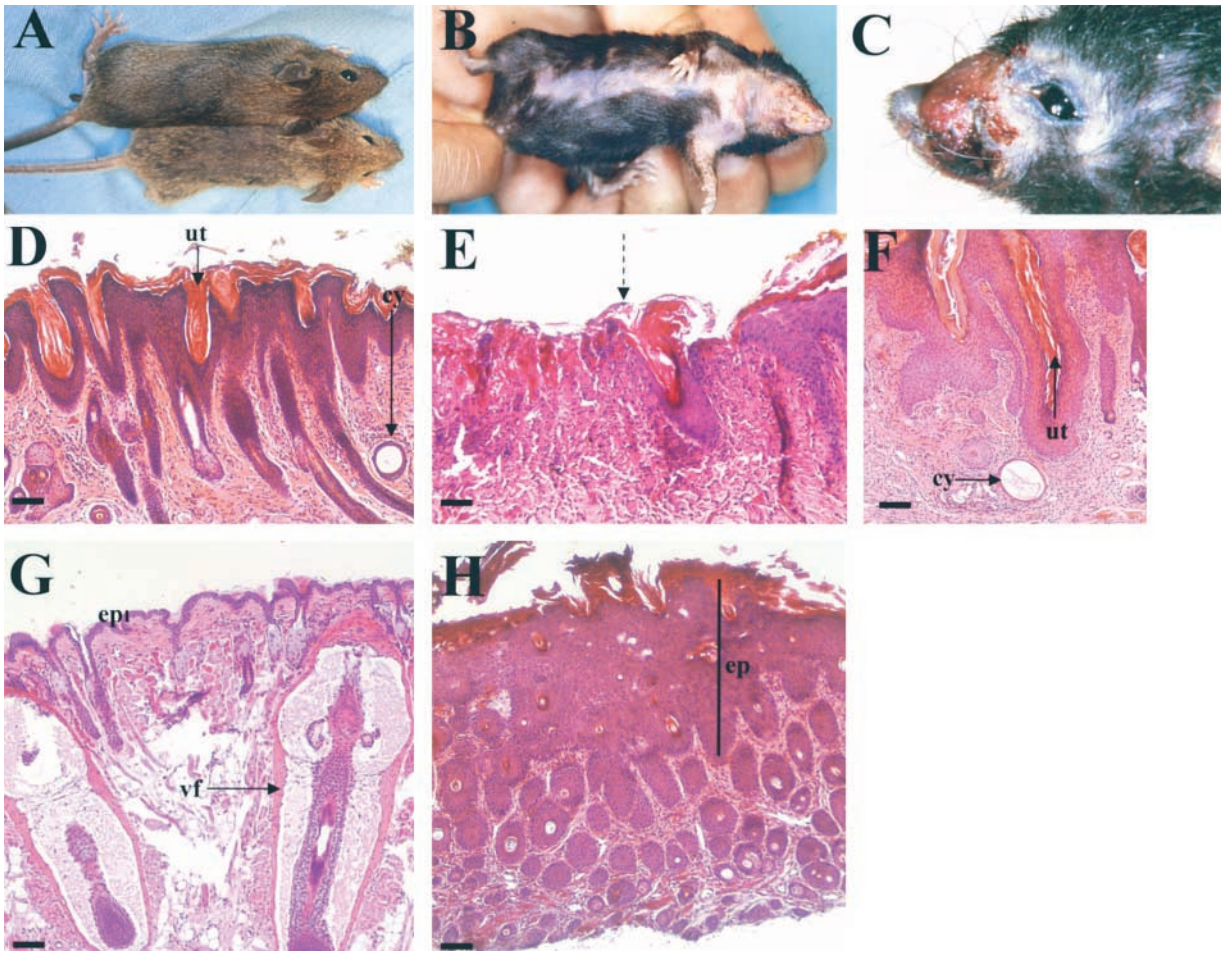

Figure 9. **Phenotype of Dsc1-null mice increases in severity with age.** (A) Scruffy and untidy coat appearance in an adult null mouse (bottom) compared with a normal littermate (top). Mice shown are 21-d-old (day of weaning). Note that the null mouse is smaller. (B) Alopecia in an adult null mouse showing the most typical pattern observed. Some ulceration on the ventral surface of the head and neck is visible also. (C) Snout ulceration in an adult null mouse showing a moderately severe example of the pattern found in all null animals and commencing after 1 mo of age. (D) Hyperplastic epidermis from the ventral surface of an adult null mouse showing acanthosis, hyperkeratosis with utriculi (ut), and cysts (cy). (E) Ulcerated skin from the abdomen of an adult Dsc1$^{-/-}$ mouse showing complete loss of epidermis from the site of the ulcer and severe inflammation. The right hand margin of the ulcer is indicated by an arrow. At this low magnification, the presence of inflammatory cells is indicated by the dermal basophilia of this region. (F) Higher magnification of a utricule (ut) and a cyst (cy). (G) Whisker pad of an adult normal mouse. vf, vibrissa follicle. (H) Whisker pad of an adult null mouse. Severe hyperplasia is present in the null as indicated by the increased number of epidermal cell layers. Approximate thickness of epidermis indicated by bars (ep) in G and H. Bars: (D, E, and G) 150 μm; (F) 25 μm.

Epidermal barrier function is compromised in neonatal *Dsc1*$^{-/-}$ mice. The defect appears to arise as a consequence of localized acantholysis and thus does not imply a direct role for Dsc1 in barrier formation, although we cannot completely exclude the possibility of a slight, more generalized defect. The effect is clearly mild and not life threatening. However, the slight reduction in epidermal barrier function and increase in water loss may cause stress to null mice and result in growth retardation. Area measurements of water and mannitol permeability and TEWL indicate a decrease in barrier function of less than twofold. A fourfold increase in TEWL is not lethal in mice transgenic for COOH-terminally truncated loricrin (Suga et al., 2000). By contrast, a targeted mutation in the keratin 10 gene results in an eightfold increase in TEWL and neonatal death (Jensen et al., 2000). Mice deficient in the cornified envelope proteins involucrin and loricrin exhibit no neonatal barrier defect, although the latter show delayed barrier formation before birth (Dijan et al., 2000; Koch et al., 2000). Therefore, these mice are affected less severely than *Dsc1*$^{-/-}$ mice.

Clear evidence for hyperproliferation and epidermal thickening was found in *Dsc1*$^{-/-}$ mice. Hyperproliferation may be a response to damage to the skin barrier. Underlying cells can sense defects in cells above and respond by proliferating in several experimental situations. Disruption of the barrier elicits DNA synthesis and epidermal hyperplasia (Proksch et al., 1991; Denda et al., 1998), and expression of the *whn* gene and NH_2-terminally truncated Dsg3 in suprabasal layers of transgenic mouse epidermis leads to both hyperproliferation and an immune response (Allen et al., 1996; Prowse et al., 1999). However, the major barrier defect in *Dsc1*$^{-/-}$ mice is localized, whereas the hyperproliferation and epidermal thickening is not. Thus, it seems likely that alterations in the program of keratinocyte terminal differentiation occur in the absence of Dsc1. Two pieces of evidence support this view. First, proliferating keratinocytes were

found in suprabasal layers of null epidermis, and second, parakeratosis was found, suggesting that the later stages of differentiation are delayed. Furthermore, there is evidence to suggest that expression of K6 and K16 in interfollicular epidermis is associated with alterations in differentiation rather than hyperproliferation (Schermer et al., 1989; Sellhayer et al., 1993; Porter et al., 1998b). However, the whole question of whether the effects we observe are a primary consequence of loss of Dsc1 or a secondary consequence of acantholysis and wound healing is a complex one that will form the subject of further investigation.

Epidermal hyperproliferation may suggest a resemblance to the common human skin disease psoriasis. However, the changes in differentiation and skin inflammation are less severe than in psoriasis, and other features, such as loss of the granular layer, formation of deep rete pegs, and dilation of dermal blood vessels, are absent.

Hair loss in *Dsc1*$^{-/-}$ mice differs from that in Dsg3-null animals. In the latter, hair loss occurs in wave-like patterns as the result of defective cell adhesion in the telogen phase of the hair cycle (Koch et al., 1998). Dsc1 is expressed in inner cell layers of the hair follicle (Chidgey et al., 1997; King et al., 1997), but despite extensive examination we found no abnormalities in timing of the hair cycle or in structure of hair follicles in *Dsc1*$^{-/-}$ mice of up to 4 wk of age. Hair loss occurred generally in older animals and was often associated with loss of normal hair follicle morphology and the presence of comedo-like structures (utriculi) and dermal cysts. Such structures characteristically result from hair follicle degeneration (Montagna et al., 1952; Mann, 1971; Panteleyev et al., 1998). Further work will be required to determine whether hair follicle degeneration is an indirect consequence of the hyperproliferative and inflammatory environment or whether Dsc1 has a role in the maintenance of normal follicle morphology.

In conclusion, the phenotype of *Dsc1*$^{-/-}$ mice demonstrates a role for this desmosomal glycoprotein in keratinocyte adhesion in the upper epidermis and in the normal function of the skin. Furthermore, our data suggest that Dsc1 contributes to the regulation of epidermal differentiation, and *Dsc1*$^{-/-}$ mice may prove useful in determining the role of desmosomes in skin disease.

Materials and methods

Isolation and characterization of the mouse *Dsc1* gene

Mouse 129SVJ λFixII (Stratagene) and PAC (RPCI21; UK HGMP Resource Centre) genomic libraries were screened with overlapping fragments of the mouse Dsc1 cDNA. Two unique nonoverlapping λ clones (λC1 and λC4) and one PAC clone (364c17) were characterized in detail. Intron sizes were determined by generating PCR products using synthetic oligonucleotide primers based on flanking exon sequences derived from the Dsc1 cDNA sequence (King et al., 1996). Exon-intron boundaries were determined by DNA sequencing and comparison with cDNA sequence.

Construction of a targeting vector and generation of Dsc1-null mice

To construct a targeting vector, a PvuII fragment from λC1, comprising 2.1 kb of DNA 5′ of the *Dsc1* initiation codon, was cloned upstream of a neomycin resistance gene under the control of a phosphoglycerate kinase promoter (Fig. 2 A). A 5.2-kb NotI (from the λFixII vector) to HindIII fragment from λC4, containing exons 2–5 of *Dsc1*, was cloned downstream of the neo gene. Vector DNA was linearized and electroporated into ES cells. Neomycin-resistant clones were isolated and screened by Southern blot analysis using BamHI-digested genomic DNA and a probe (1 kb), which hybridized to DNA 5′ to the homologous sequences used in the targeting vector (Fig. 2 A). One recombinant ES cell clone was injected into C57Bl/6J blastocysts, and the resulting chimeric male offspring were mated with female C57Bl/6J mice. Tail DNA from agouti offspring was tested for the presence of the mutated allele by Southern blot hybridization. Heterozygous mice were intercrossed to obtain mice, which were homozygous for the *Dsc1*-null allele.

RT-PCR

Newborn (2-d-old) mice were killed, and their skin was removed and immersed in 5 mM EDTA in PBS for 3 min at 50°C. The epidermis was peeled from the dermis, homogenized in Trizol reagent, and total RNA was prepared according to the manufacturer's instructions (Life Technologies). First strand cDNA synthesis was performed from RNA using a kit (Roche) and random primers. An aliquot (1 μl) of the first strand cDNA reaction was amplified using primers P1 (AGGGAGCACCTTCTCTAAGCAG) and P2 (AAGGCTCTTTGTCTACTCCTGG), specific for exons 1 and 5, respectively, and P3 (GGTCCATTTCCACAACACATT) and P4 (TGTACTTCAGACGAGTGTGTA), specific for exons 4 and 7, respectively. Glyceraldehyde-3-phosphate dehydrogenase primers (CLONTECH Laboratories, Inc.) were added to PCR reactions as a positive control.

Western blotting

Epidermis was isolated from 2-d-old mice as above and dissolved in sample buffer. Proteins were separated by SDS-polyacrylamide gel electrophoresis and transferred to polyvinylidene difluoride membrane (Amersham Pharmacia Biotech). Primary antibodies were JCMC (1:10,000) against Dsc1 (North et al., 1996), JB1 (1:500) against Dsc2 (Hyam, J.L.M., personal communication), rabbit anti–mouse Dsc3 (1:100; unpublished data; Liu, K., and D. Marshall, personal communication), DG3.10 (1:100) against Dsg1+2 (Progen), mouse anti–human PG (1:5,000; Transduction Laboratories), and 11–5F (1:40) against DP (Parrish et al., 1987). Primary antibodies were detected using appropriate peroxidase-conjugated secondary antibodies and the ECL detection system (Amersham Pharmacia Biotech).

Histological and immunochemical analysis

For histological analysis, tissues were fixed routinely in formol saline, embedded in paraffin, and stained with hematoxylin and eosin. Cell proliferation was examined in paraffin sections by staining for Ki67 (Gerdes et al., 1984). Expression of desmosomal constituents and differentiation markers were examined in frozen sections. Tissue was embedded in cryoprotectant (OCT; Miles), frozen in liquid nitrogen, and cryosections fixed in ice-cold methanol (5 min). Primary antibodies were JCMC (1:500), PAT-C (1:10) against Dsc2 (Messent et al., 2000), DG3.10 (1:50), PG-11E4 (1:100) against PG (Zymed Laboratories), 11–5F (1:25), MK1 (1:2,500) against keratin 1 (Covance), MK6 (1:2,500) against keratin 6 (Covance), MK14 (1:20,000) against keratin 14 (Covance), RPmK16 (1:500) against keratin 16 (Porter et al., 1998a), rat anti–mouse β_4 integrin (10 μg/ml; Pharmingen), PCD-1 (10 μg/ml) against P-cadherin (R & D Systems), rabbit antiinvolucrin (1:100; Covance), and rabbit antifilaggrin (1:1,000; Covance). Primary antibodies were detected with the appropriate FITC-conjugated secondary antibodies. Sections were examined using an Olympus BX49 microscope.

EM

Fresh skin was dissected into small pieces (~1 × 1 × 0.5 mm) and fixed by immersion in 2% formaldehyde (freshly made from paraformaldehyde powder) plus 2% glutaraldehyde in 0.1 M sodium cacodylate buffer (pH 7.3). Tissues were fixed for 2 h at room temperature and then washed four times with cacodylate buffer. They were then post-fixed with 1% osmium tetroxide for 2 h, dehydrated through an ethanol series, and embedded in Spurr's resin. Ultrathin sections were contrasted with uranyl acetate and lead citrate and examined on a Philips 400 electron microscope.

Analysis of skin barrier function

Dye penetration assays. These were performed as described by Hardman et al. (1998) and Marshall et al. (2000).

Passive diffusion of solutes. Samples of mouse back skin were clamped in continuous flow-through perfusion chambers. $^{3}H_2O$ (5 μCi/ml) and [^{14}C]mannitol (0.1 μCi/ml) were added to the donor compartment, and PBS (4 ml/h) was passed across the connective tissue side and collected hourly for up to 18 h. Samples were counted in a Beckman LS 6000 liquid scintillation counter, and a steady-state permeability constant (Kp) was determined in units of cm/min (Healy et al., 2000; Selvaratnam et al., 2001). Experiments were performed at 32°C.

TEWL. This was determined using a Tewameter (Courage and Khazaka). After decapitation or halothane anesthesia, a probe (1 cm diameter) was applied to the back of 2-d-old animals, and measurements of 1-min duration were taken.

Cornified envelope preparation

Epidermis from 2-d-old mice (see above) was heated to 95°C for 10 min in extraction buffer (0.1 M Tris-HCl, pH 8.5, 2% SDS, 20 mM dithiothreitol, and 5 mM EDTA), and the cornified envelopes were collected by centrifugation at 5,000 *g* for 15 min. The extraction was repeated once, and the envelopes were resuspended and stored in extraction buffer.

We are grateful to Dr. S. Andrew, Dr. E. Bell, Professor C.M. Griffiths, Dr. M. Hardman, Professor T. Hashimoto, Mr. D. Marshall, Mr. G. Morrissey, Mrs. J. Morrissey, and Miss Anjana Patel for help and advice.

The work was supported by the Wellcome Trust, Medical Research Council, and Royal Society.

Submitted: 1 May 2001
Revised: 22 August 2001
Accepted: 15 October 2001

References

Allen, E., Q.-C. Yu, and E. Fuchs. 1996. Mice expressing a mutant desmosomal cadherin exhibit abnormalities in desmosomes, proliferation, and epidermal differentiation. *J. Cell Biol.* 133:1367–1382.

Amagai, M. 1999. Autoimmunity against desmosomal cadherins in pemphigus. *J. Dermatol. Sci.* 20:92–102.

Amagai, M., K. Tsunoda, H. Suzuki, K. Nishifuji, S. Koyasu, and T. Nishikawa. 2000. Use of autoantigen-knockout mice in developing an active autoimmune disease model for pemphigus. *J. Clin. Invest.* 105:625–631.

Buxton, R.S., P. Cowin, W.W. Franke, D.R. Garrod, K.J. Green, I.A. King, P.J. Koch, A.I. Magee, D.A. Rees, J.R. Stanley, et al. 1993. Nomenclature of the desmosomal cadherins. *J. Cell Biol.* 121:481–483.

Charpentier, E., R.M. Lavker, E. Acquista, and P. Cowin. 2000. Plakoglobin suppresses epithelial proliferation and hair growth in vivo. *J. Cell Biol.* 149:503–519.

Chidgey, M.A.J., K.K.M. Yue, S. Gould, C. Byrne, and D.R. Garrod. 1997. Changing pattern of desmocollin 3 expression accompanies epidermal organisation during skin development. *Dev. Dyn.* 210:315–327.

Chitaev, N.A., and S.M. Troyanovsky. 1997. Direct Ca^{2+}-dependent heterophilic interaction between desmosomal cadherins, desmoglein and desmocollin, contributes to cell–cell adhesion. *J. Cell Biol.* 138:193–201.

Collins, J.E., P.K. Legan, T.P. Kenny, J. MacGarvie, J.L. Holton, and D.R. Garrod. 1991. Cloning and sequence analysis of desmosomal glycoproteins 2 and 3 (desmocollins): cadherin-like desmosomal adhesion molecules with heterogeneous cytoplasmic domains. *J. Cell Biol.* 113:381–391.

Denda, M., J. Sato, T. Tsuchiya, P.M. Elias, and K.R. Feingold. 1998. Low humidity stimulates epidermal DNA synthesis and amplifies the hyperproliferative response to barrier disruption: implication for seasonal exacerbations of inflammatory dermatoses. *J. Invest. Dermatol.* 111:873–878.

Dijan, P., K. Easley, and H. Green. 2000. Targeted ablation of the murine involucrin gene. *J. Cell Biol.* 151:381–387.

Garrod, D.R. 1995. Desmosomes and cancer. *In* Cancer Surveys. Vol. 24. Cell adhesion and cancer. I. Hart and N. Hogg, editors. Cold Spring Harbor Laboratory Press, New York. 97–111.

Garrod, D., M. Chidgey, and A. North. 1996. Desmosomes: differentiation, development, dynamics and disease. *Curr. Opin. Cell Biol.* 8:670–678.

Gerdes, J., H. Lemke, H. Baisch, H.H. Wacker, U. Schwab, and H. Stein. 1984. Cell cycle analysis of a cell proliferation-associated human nuclear antigen defined by the monoclonal antibody Ki-67. *J. Immunol.* 133:1710–1715.

Green, K.J., and C.A. Gaudry. 2000. Are desmosomes more than tethers for intermediate filaments? *Nat. Rev. Mol. Cell Biol.* 1:208–216.

Greenwood, M.D., M.D. Marsden, C.M.E. Cowley, V.K. Sahota, and R.S. Buxton. 1997. Exon-intron organisation of the human type 2 desmocollin gene (DSC2): desmocollin gene structure is closer to "classical" cadherins than to desmogleins. *Genomics.* 44:330–335.

Hardman, M.J., P. Sisi, D.N. Banbury, and C. Byrne. 1998. Patterned acquisition of skin barrier function during development. *Development.* 125:1541–1552.

Hashimoto, T., C. Kiyokawa, O. Mori, M. Miyasato, M.A.J. Chidgey, D.R. Garrod, Y. Kobayashi, K. Komori, K. Ishii, M. Amagai, et al. 1997. Human desmocollin 1 (Dsc1) is an autoantigen for the subcorneal pustular dermatosis type of IgA pemphigus. *J. Invest. Dermatol.* 109:127–131.

Hatzfeld, M. 1999. The armadillo family of structural proteins. *Int. Rev. Cytol.* 186:179–224.

Healy, C.M., A.T. Cruchley, M.H. Thornhill, and D.M. Williams. 2000. The effect of sodium lauryl sulphate, triclosan and zinc on the permeability of normal oral mucosa. *Oral Diseases.* 6:118–123.

Hunt, D.M., V.K. Sahota, K. Taylor, D. Simrak, N. Hornigold, J. Arnemann, J. Wolfe, and R.S. Buxton. 1999. Clustered cadherin genes: a sequence-ready contig for the desmosomal cadherin locus on human chromosome 18. *Genomics.* 62:445–455.

Jensen, J.-M., S. Schütze, C. Neumann, and E. Proksch. 2000. Impaired cutaneous permeability barrier function, skin hydration, and sphingomyelinase activity in keratin 10 deficient mice. *J. Invest. Dermatol.* 115:708–713.

King, I.A., T.J. O'Brien, and R.S. Buxton. 1996. Expression of the "skin-type" desmosomal cadherin DSC1 is closely linked to the keratinization of epithelial tissues during mouse development. *J. Invest. Dermatol.* 107:531–538.

King, I.A., B.D. Angst, D.M. Hunt, M. Kruger, J. Arnemann, and R.S. Buxton. 1997. Hierarchical expression of desmosomal cadherins during stratified epithelial morphogenesis in the mouse. *Differentiation.* 62:83–96.

Koch, P.J., M.G. Mahoney, H. Ishikawa, L. Pulkkinen, J. Uitto, L. Shultz, G.F. Murphy. D. Whitaker-Menezes, and J.R. Stanley. 1997. Targeted disruption of the pemphigus vulgaris antigen (desmoglein 3) gene in mice causes loss of keratinocyte cell adhesion with a phenotype similar to pemphigus vulgaris. *J. Cell Biol.* 137:1091–1102.

Koch, P.J., M.G. Mahoney, G. Cotsarelis, K. Rothenberger, R.M. Lavker, and J.R. Stanley. 1998. Desmoglein 3 anchors telogen hair in the follicle. *J. Cell Sci.* 111:2529–2537.

Koch, P.J., P.A. de Viragh, E. Scharer, D. Bundman, M.A. Longley, J. Bickenbach, Y. Kawachi, Y. Suga, Z. Zhou, M. Huber, et al. 2000. Lessons from loricrin-deficient mice: compensatory mechanisms maintaining skin barrier function in the absence of a major cornified envelope protein. *J. Cell Biol.* 151:389–400.

Legan, P.K., K.K.M. Yue, M.A.J. Chidgey, J.L. Holton, R.W. Wilkinson, and D.R. Garrod. 1994. The bovine desmocollin family: a new gene and expression patterns reflecting epithelial cell proliferation and differentiation. *J. Cell Biol.* 126:507–518.

Mahoney, M.G., Z. Wang, K. Rothenberger, P.J. Koch, M. Amagai, and J.R. Stanley. 1999. Explanation for the clinical and microscopic localization of lesions in pemphigus foliaceus and vulgaris. *J. Clin. Invest.* 103:461–468.

Mann, S.J. 1971. Hair loss and cyst formation in hairless and rhino mutant mice. *Anat. Rec.* 170:485–500.

Marcozzi, C., I.D.J. Burdett, R.S. Buxton, and A.I. Magee. 1998. Coexpression of both types of desmosomal cadherin and plakoglobin confers strong intercellular adhesion. *J. Cell Sci.* 111:495–509.

Marshall, D., M.J. Hardman, and C. Byrne. 2000. SPRR1 gene induction and barrier formation occur as coordinated moving fronts in terminally differentiating epithelia. *J. Invest. Dermatol.* 114:967–975.

Messent, A.J., M.J. Blisset, G.L. Smith, A.J. North, A. Magee, D. Foreman, D.R. Garrod, and M. Boulton. 2000. Expression of a single pair of desmosomal glycoproteins renders the corneal epithelium unique amongst stratified epithelia. *Invest. Ophthalmol. Vis. Sci.* 41:8–15.

Montagna, W., H.B. Chase, and H.P. Melarango. 1952. The skin of hairless mice. The formation of cysts and the distribution of lipids. *J. Invest. Dermatol.* 19: 83–94.

North, A.J., M.A.J. Chidgey, J.P. Clarke, W.G. Bardsley, and D.R. Garrod. 1996. Distinct desmocollin isoforms occur in the same desmosomes and show reciprocally graded distributions in bovine nasal epidermis. *Proc. Natl. Acad. Sci. USA.* 93:7701–7705.

Nuber, U.A., S. Schafer, S. Stehr, H.-R. Rackwitz, and W.W. Franke. 1996. Patterns of desmocollin synthesis in human epithelia: immunolocalization of desmocollins 1 and 3 in special epithelia and in cultured cells. *Eur. J. Cell Biol.* 71:1–13.

Osada, K., M. Seishima, and Y. Kitajima. 1997. Pemphigus IgG activates and translocates protein kinase C from the cytosol to the particulate/cytoskeleton fractions in human keratinocytes. *J. Invest. Dermatol.* 108:482–487.

Panteleyev, A.A., C. van der Veen, T. Rosenbach, S. Müller-Röver, V. Sokolov, and R. Paus. 1998. Towards defining the pathogenesis of the *hairless* phenotype. *J. Invest. Dermatol.* 110:902–907.

Parrish, E.P., P.V. Steart, D.R. Garrod, and R.O. Weller. 1987. Antidesmosomal monoclonal antibody in the diagnosis of intracranial tumors. *J. Pathol.* 153: 265–273.

Porter, R.M., A.M. Hutcheson, E.L. Rugg, R.A. Quinlan, and E.B. Lane. 1998a. cDNA cloning, expression, and assembly characteristics of mouse keratin 16.

J. Biol. Chem. 273:32265–32272.

Porter, R.M., J. Reichelt, D.P. Lunny, T.M. Magin, and E.B. Lane. 1998b. The relationship between hyperproliferation and epidermal thickening in a mouse model for BCIE. *J. Invest. Dermatol.* 110:951–957.

Proksch, E., K.R. Feingold, M. Mao-Qiang, and P.M. Elias. 1991. Barrier function regulates epidermal DNA synthesis. *J. Clin. Invest.* 87:1668–1673.

Prowse, D.M., D. Lee, L. Weiner, N. Jiang, C.M. Magro, H.P. Baden, and J.L. Brissette. 1999. Ectopic expression of the *nude* gene induces hyperproliferation and defects in differentiation: implications for the self-renewal of cutaneous epithelia. *Devl. Biol.* 212:54–67.

Robinson, N.A., S. Lapic, J.F. Welter, and R.L. Eckert. 1997. S100A11, S100A10, annexin1, desmosomal proteins, small proline-rich proteins, plasminogen activator inhibitor-2, and involucrin are components of the cornified envelope of cultured human epidermal keratinocytes. *J. Biol. Chem*. 272:12035–12046.

Schermer, A., J.V. Jester, C. Hardy, D. Milano, and T.-T. Sun. 1989. Transient synthesis of K6 and K16 keratins in regenerating rabbit corneal epithelium: keratin markers for an alternative pathway of keratinocyte differentiation. *Differentiation.* 42:103–110.

Sellhayer, K., J.B. Bickenbach, J.A. Rothnagel, D. Bundman, M.A. Longley, T. Krieg, N.S. Roche, A.B. Roberts, and D.R. Roop. 1993. Inhibition of skin development by overexpression of transforming growth factor β_1 in the epidermis of transgenic mice. *Proc. Natl. Acad. Sci. USA.* 90:5237–5241.

Selvaratnam, L., A.T. Cruchley, H. Navsaria, P. Wertz, E. Hagi-Pavli, I.M. Leigh, C.A. Squier, and D.M. Williams. 2001. Oral keratinocytes develop a functional and biochemical permeability barrier similar to intact oral mucosa. *Oral Diseases.* 7:252–258.

Shimizu, H., T. Masunaga, A. Ishiko, A. Kikuchi, T. Hashimoto, and T. Nishikawa. 1995. Pemphigus vulgaris and pemphigus foliaceus sera show an inversely graded binding pattern to extracellular regions of desmosomes in different layers of human epidermis. *J. Invest. Dermatol.* 105:153–159.

Shinohara, M., A. Hiraki, T. Ikebe, S. Nakamura, S.-I. Kurahara, K. Shirasuna, and D.R. Garrod. 1998. Immunohistochemical study of desmosomes in oral squamous cell carcinoma: correlation with cytokeratin and E-cadherin staining, and with tumour behaviour. *J. Pathol.* 184:369–381.

Suga, Y., M. Jarmick, P.S. Attar, M.A. Longley, D. Bundman, A.C. Steven, P.J. Koch, and D.R. Roop. 2000. Transgenic mice expressing a mutatant form of loricrin reveal the molecular basis of the skin diseases, Vohwinkel syndrome and progressive symmetric erythrokeratoderma. *J. Cell Biol.* 151: 401–412.

Tselepis, C., M. Chidgey, A. North, and D. Garrod. 1998. Desmosomal adhesion inhibits invasive behavior. *Proc. Natl. Acad. Sci. USA.* 95:8064–8069.

Wallis, S., S. Lloyd, I. Wise, G. Ireland, T.P. Fleming, and D. Garrod. 2000. The α isoform of protein kinase C is involved in signaling the response of desmosomes to wounding in cultured epithelial cells. *Mol. Biol. Cell.* 11:1077–1092.

Whitby, D.J., and M.W.J. Ferguson. 1991. The extracellular matrix of lip wounds in fetal, neonatal and adult mice. *Development.* 112:651–668.

Whittock, N.V., D.M. Hunt, L. Rickman, S. Malhi, A.P. Vogazianou, L.F Dawson, R.A.J. Eady, R.S Buxton, and J.A. McGrath. 2000. Genomic organisation and amplification of the human desmosomal cadherin genes *DSC1* and *DSC3,* encoding desmocollin types 1 and 3. *Biochem. Biophys Res. Comm.* 276:455–460.